

# Molecular magnets

## Hybrid organic–inorganic layered compounds with very long-range ferromagnetism

V. Laget <sup>a</sup>, C. Hornick <sup>a</sup>, P. Rabu <sup>a</sup>, M. Drillon <sup>a,\*</sup>, R. Ziessel <sup>b</sup>

<sup>a</sup> *Institut de Physique et Chimie des Matériaux, UMR 46 du CNRS, 23 rue du Loess, 67037 Strasbourg, France*

<sup>b</sup> *Laboratoire de Chimie, d'Electronique et de Photonique Moléculaire, ECPM, UPRES-A 7008 du CNRS, 1 rue Blaise Pascal, 67008 Strasbourg, France*

Received 27 January 1998; accepted 11 May 1998

### Contents

Abstract	1533
1. Introduction	1534
2. Layered magnetic systems	1535
3. Influence of organic spacers	1538
4. Very long range ferromagnetic order	1545
5. Metal-radical layered magnets	1549
6. Concluding remarks	1552
Acknowledgements	1552
References	1552

### Abstract

The correlations between structures and magnetic properties of new hybrid layered compounds  $M_2(OH)_3X$  ( $M = Co$  or  $Cu$ ), where  $X$  is an exchangeable organic anion, are investigated. When the anion is a simple spacer (aliphatic chain), ferromagnetic in-plane interactions dominate, and the situation depends to a large extent on the interlayer spacing  $d$ . For small spacings ( $d < 10 \text{ \AA}$ ), 3D antiferromagnetic order is stabilized, while large spacings favor spontaneous magnetization, even for  $d \approx 40 \text{ \AA}$ , due to dipolar through-space interactions. When  $X$  is a radical anion, new metal-radical magnets, with  $d$  close to  $20 \text{ \AA}$ , are achieved. Strong interactions between the 3d and  $\pi$  electrons are evidenced, and a net magnetic moment occurs at low temperature. Such compounds are promising for the design of new molecular multiproperty materials. © 1998 Elsevier Science S.A. All rights reserved.

**Keywords:** Dipolar interactions; Hybrid magnets; Molecular magnetism; Organic spacers; Radical-based magnets

\* Corresponding author. Fax: +33 3 88107250; e-mail: drillon@teutates.u-strasbg.f2

## 1. Introduction

Molecule-based compounds exhibiting ferromagnetic properties have attracted continuous interest in recent years [1–3]. The ability of molecular chemists to produce a large variety of organic or organometallic building blocks is used to build new magnetic arrays. The strategy consists of assembling the building units in a controllable fashion, in order to promote ferromagnetic exchange interactions between nearest neighbors. Indeed, as far as the spin carriers are close to each other, the exchange coupling is related to the symmetry of the magnetic orbitals or the spin polarization effects. In parallel, solid state chemists have focused on extended magnetic compounds, in particular on low-dimensional systems which exhibit physical properties not available in 3D compounds.

Recently, a novel trend of investigation has been the combination of both molecular and solid state chemistry to isolate hybrid systems. Pioneering work on metal–radical polynuclear complexes has shown that a significant exchange coupling may occur between the two spin carriers [4,5]. Further, research on organic–inorganic compounds is very appealing for the design of novel 3D architectures in which the physical properties of both assemblies are closely related. Striking results have been obtained in photo-induced magnetic and conducting materials [6,7], and in systems combining two basic properties, conductivity and magnetism or optics and magnetism for instance [8,9].

In this way, the chemistry of layered compounds is well adapted for the design of such new hybrid materials with outstanding magnetic properties [10–17]. For example, the layered hydroxide nitrates  $M_2(OH)_3(NO_3)$  where  $M = Co, Ni, Cu$ , exhibit, like the parent hydroxide  $\beta\text{-}M(OH)_2$  compounds, a 2D triangular array of the metal ions.  $[M_2(O_H)_3O_N]$  layers hold together through hydrogen bonds, involving hydroxyl ions and oxygen atoms of nitrate groups (Fig. 1). The metal ions are coordinated either to four equatorial  $(OH)^-$  and two oxygen atoms belonging to  $(NO_3)^-$ , or to five  $(OH)^-$  and one  $(NO_3)^-$  in an axial position. Replacing one in four of the hydroxyl ions by nitrate groups induces a significant enhancement of the basal spacing from 4.65 Å for the hydroxide to 6.96 Å for the hydroxide nitrate. In turn, the lattice dimensions in the  $a$ – $b$  plane remain unchanged.

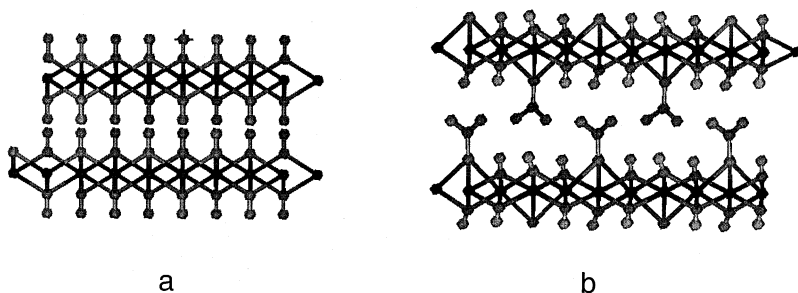


Fig. 1. Layered structures of the hydroxide  $M(OH)_2$  (a) and hydroxide nitrate  $M_2(OH)_3(NO_3)$  (b).

We describe hereafter how these systems provide good examples of planar triangular magnetic arrays, and how their properties are closely related to the in-plane and interplane magnetic exchange interactions.

From these compounds, new hybrid magnetic materials have been prepared by anion exchange reaction. Exchange reactions are well known in smectite clays or layered double hydroxides (LDHs)  $[M_{1-x}^{II}M_x^{III}(\text{OH})_2]^+A_x^-$  [18–20]. In the latter, organic as well as inorganic anions (A) are located between the hydroxide layers, counter-balancing the positive charge due to the substitution of divalent by trivalent metal ions. Recently, Yamanaka et al. [21] have investigated the exchange reactions in the layered copper(II) compound  $\text{Cu}_2(\text{OH})_3(\text{CH}_3\text{COO})\cdot\text{H}_2\text{O}$  in order to prepare highly active oxidation catalysts. It was demonstrated that the acetate anion located in the interlayer space may easily be substituted by halides,  $\text{NO}_3^-$ ,  $\text{ClO}_4^-$  anions and even by transition-metal complexes.

The layered compounds  $M_2(\text{OH})_3X$  (with  $M = \text{Co}, \text{Cu}$ ), in which the exchangeable anion  $X = \text{NO}_3^-$  or  $\text{OAc}^-$  is coordinated to the divalent metal ion, are well adapted for substitution reactions [18,21]. The use of large organic species (*n*-alkyl sulfates or *n*-alkyl carboxylates) for the substitution of  $X$  enables us to tune the basal spacing, and accordingly to control the magnetic dimensionality [14–17]. These compounds show similarities with the extensively studied copper(II) weak ferromagnets,  $\text{CuCl}_4(\text{C}_n\text{H}_{2n+1}\text{NH}_3)_2$ , in which the influence of the interlayer distance on the magnetic behavior has been evidenced [22].

Finally, we will show that anionic exchange reactions are available with organic radical anions, giving new hybrid ferromagnets  $\text{Co}_2(\text{OH})_{3.5}(\text{IMB})_{0.5}\cdot 2\text{H}_2\text{O}$  (IMB = imino-nitroxide benzoate anion). In these systems, the metal layers are interleaved with radical anions, and the two subunits are strongly coupled through covalent bonds. Such novel compounds may be viewed as supramolecular multilayer magnets, and may be compared to the classical ferromagnetic metal-based superlattices.

## 2. Layered magnetic systems

Let us first consider the magneto-structural correlations in the layered cobalt(II) hydroxide and hydroxide nitrate, which may be considered as good prototypes of two-dimensional ferromagnetic systems [23].

The in-plane  $\text{Co(II)}-\text{Co(II)}$  distances, related to *a* (or *b*) parameters, are identical in both structures, while the periodicity *c* of the stacking differs significantly (factor 1.5). The essential difference between these two compounds is a larger distance between successive  $\text{Co(II)}$  layers in  $\text{Co}_2(\text{NO}_3)(\text{OH})_3$  with respect to  $\text{Co(OH)}_2$  (Fig. 1).

The temperature dependence of the magnetic susceptibility and high field magnetization of  $\text{Co}_2(\text{OH})_3(\text{NO}_3)$  are plotted in Fig. 2, and compared to the parent compound  $\text{Co(OH)}_2$  [23]. The  $\chi T$  product exhibits, upon cooling, a slight decrease down to 40 K, due to the spin–orbit coupling effect stabilizing a Kramers doublet for  $\text{Co(II)}$  ion, then a significant increase up to a sharp maximum (for  $T = 9.8$  K), and a drop to zero on further cooling. Such behavior is characteristic of ferromag-

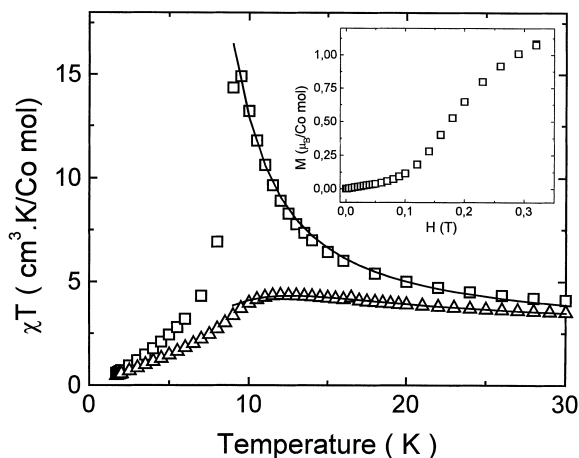


Fig. 2. Magnetic behaviors of  $\text{Co}(\text{OH})_2$  (triangles) and  $\text{Co}_2(\text{OH})_3(\text{NO}_3)$  (squares), illustrated as plots of  $\chi T = f(T)$  and  $M = f(H)$  (in the inset).

netic in-plane interactions between cobalt(II) ions. Field dependent magnetization measurements (Fig. 2) show a typical metamagnetic transition in the ordered state for  $H_c = 0.17$  T, and a saturation at  $\sim 2.87\mu_B$ , in agreement with the expected value. A similar behavior is observed for  $\text{Co}(\text{OH})_2$  [23,24].

Specific heat measurements exhibit, for both compounds, an anomalous peak at 11.6 K ( $\pm 0.2$  K) for the hydroxide and 8.7 K ( $\pm 0.1$  K) for the hydroxide nitrate. By comparison with the magnetic findings (10.0 K and 9.8 K, respectively), these peaks may be related to the stabilization of a long-range magnetic ordering. The results for  $\text{Co}(\text{OH})_2$  agree well with those of Soraï et al. ( $\lambda$ -type anomaly at 11.6 K) [25].

Clearly, the magnetic results indicate for both compounds two regimes, corresponding to short-range ( $T > T_c$ ) and long-range ( $T < T_c$ ) magnetic correlations between cobalt(II) ions. At high temperature, ferromagnetic in-plane interactions dominate the magnetic properties, as evidenced by the sharp increase of  $\chi T$  when approaching the ordering temperature. Thus, these compounds may be viewed as good prototypes of 2D triangular ferromagnets, the properties of which closely depend on the spin dimensionality. At low temperature, an important feature concerns the lattice dimensionality. Some insights are given in the following discussion.

As a result of the combined action of crystal-field and spin-orbit coupling, the lowest multiplet of Co(II) is well approximated by an effective spin  $S = 1/2$ , with highly anisotropic properties. An analysis of the low-dimensional behavior can be performed for both Co(II) compounds on the basis of the  $S = 1/2$  2D Ising model. The influence of interlayer interactions ( $z_j$ ) is introduced by use of the mean field approximation. Clearly, the interaction between adjacent layers depends on the interlayer distance, namely the  $c$  parameter, so that it is expected to be more efficient for  $\text{Co}(\text{OH})_2$  than for  $\text{Co}_2(\text{OH})_3(\text{NO}_3)$ . In this approximation, a very good descrip-

Table 1

Values of magnetic parameters obtained from high temperature series expansion [26]

Compound	Dimensionality	$g$	$J$ (K)	$zj$ (K)
$\text{Co}(\text{OH})_2$	2D/3D	5.09	9.2	−2.57
$\text{Co}_2(\text{OH})_3(\text{NO}_3)$	2D/3D	5.11	7.4	−0.23

tion of the magnetic susceptibility (Fig. 2) is obtained from the parameters listed in Table 1.

From the above results, it appears that the two-dimensional character is much more pronounced for  $\text{Co}_2(\text{OH})_3(\text{NO}_3)$  than for  $\text{Co}(\text{OH})_2$ , as predicted from structural data. This agrees with the field dependent magnetization measurements which show a metamagnetic behavior for both compounds, with critical fields ranging from 0.17 T for the hydroxide nitrate to 1.5 T for the hydroxide. The critical ordering temperatures are, however, very close between compounds. Indeed, if interlayer interactions are needed for the occurrence of long-range 3D ordering, the divergence of the in-plane correlation length  $\xi$  close to  $T_c$  appears to be the driving force, according to the relationship  $kT_c \sim \xi^2 JS^2$  [22].

The second example concerns the antiferromagnetic copper(II) hydroxide nitrate [14,27], isostructural with the cobalt(II) derivative. Its structure is monoclinic (space group  $P2_1$ ) with the unit cell parameters  $a=5.61$  Å,  $b=6.09$  Å,  $c=6.93$  Å,  $\beta=94.48^\circ$  [28].

The temperature dependent magnetic susceptibility (Fig. 3) shows a maximum at  $T_c=12$  K corresponding to the long-range ordering. On the other hand, the decrease of  $\chi T$  upon cooling from  $0.91 \text{ cm}^3 \text{ K mol}^{-1}$  at 150 K, down to  $4.9 \times 10^{-2} \text{ cm}^3 \text{ K mol}^{-1}$  at 1.7 K clearly provides evidence for antiferromagnetic in-plane interactions. Single crystal measurements [27] indicate the same behavior

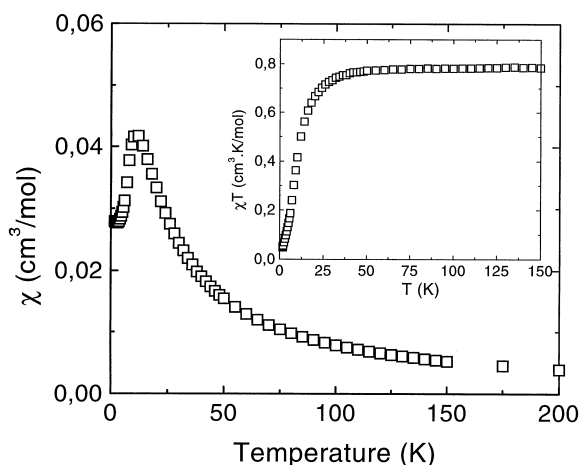


Fig. 3. Temperature dependence of the magnetic susceptibility and the  $\chi T$  product for  $\text{Cu}_2(\text{OH})_3(\text{NO}_3)$ .

without anisotropy effect, as expected for copper(II) ions. Basically, such a system may be considered as a good prototype of a frustrated Heisenberg 2D system, which from a theoretical point of view is still controversial as regards the nature of the ground-state.

The low temperature variation of  $\chi(T)$  agrees with a long-range antiferromagnetic (AF) order below  $T_c$ . However, a 3D order was not detected by neutron diffraction experiment on deuterated powder samples. As a result, it can be assumed that the maximum of susceptibility is related to short-range AF correlations within copper(II) layers.

Finally, it is indicated that transition metal hydroxide nitrates are good examples of triangular 2D magnets over a large temperature range, as long as weak interlayer interactions through hydrogen bonds are negligible [14,23,29].

The basal spacing of  $\sim 6.9$  Å is not large enough to avoid the influence of interlayer exchange interactions at low temperature. In order to minimize this influence, large organic species, such as *n*-alkyl sulfate or *n*-alkyl carboxylate anions, have been coordinated to the metal ion to enhance the interlayer spacing.

### 3. Influence of organic spacers

Consider now the influence of large coordinating species on the magnetic behavior of cobalt(II) or copper(II) compounds. The correlation structure-properties are detailed for the  $\text{Co}_2(\text{OH})_3\text{X}$  series, where X is an organic (i.e. aliphatic chain) anionic spacer coordinated to the divalent metal ion [14,15]. The results are shown to be very similar for copper(II) compounds [16,17]. In particular, it is evidenced in the following that, for large interlayer spacing, long-range ferromagnetism is stabilized due to the effect of dipolar interactions [30].

The cobalt(II) hydroxide acetate  $\text{Co}_2(\text{OH})_3(\text{CH}_3\text{CO}_2)_x \cdot z\text{H}_2\text{O}$  is prepared similarly to hydroxide nitrate<sup>1</sup>, while the hybrid compounds  $\text{Co}_2(\text{OH})_{4-x}(\text{C}_n\text{H}_{2n+1}\text{COO})_x \cdot z\text{H}_2\text{O}$  ( $n=7, 9, 10, 12$ ) and  $\text{Co}_2(\text{OH})_{4-x}(\text{C}_n\text{H}_{2n+1}\text{SO}_4)_x \cdot z\text{H}_2\text{O}$  ( $n=6, 9, 12$ ) are obtained by an anion exchange reaction. A suspension of  $\text{Co}_2(\text{OH})_3(\text{NO}_3)_2$  in aqueous solution is used as starting material, with the appropriate sodium salts of the exchangeable anion. Chemical analysis gives, for the *n*-alkyl carboxylate series,  $x=0.8 \pm 0.05$ , and for the *n*-alkyl sulfate series,  $x=0.55 \pm 0.05$ .

The X-ray powder diffraction patterns of the substituted compounds show strong (00 $l$ ) reflections, in agreement with the expected layered structures (Fig. 4) [18,19,21]. As might be anticipated, the interlayer spacing (*c* parameter) is closely related to the *n*-alkyl chain length, except for the hydroxide acetate (Fig. 5), while the in-plane parameters remain quasi-constant. All cobalt(II) *n*-alkyl compounds exhibit hexagonal symmetry with space group P3m, similar to  $\text{Co}(\text{OH})_2$ .

For  $\text{Co}_2(\text{OH})_{3.2}(\text{OAc})_{0.8} \cdot z\text{H}_2\text{O}$ , the interlayer spacing decreases from 12.7 Å

<sup>1</sup>Slow addition of an aqueous solution of NaOH (1 M) to a solution of cobalt acetate at 90 °C, with a Co:Na ratio of less than 1.5. The resulting precipitate is filtered and washed with acetone, then dried under vacuum. The anhydrous form is obtained by heating the former at 80 °C for 24 h.

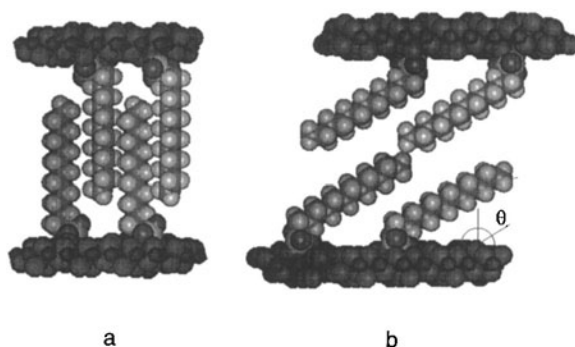


Fig. 4. Structural model for layered *n*-alkyl compounds exhibiting single-layer (a) and double-layer (b) chains separating metal-based inorganic layers.

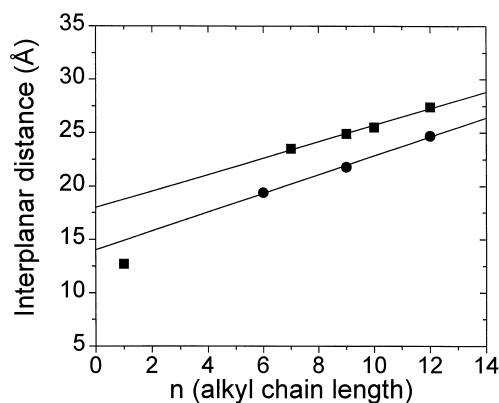


Fig. 5. Variation of the interlayer spacing as a function of *n* (number of carbon atoms) in cobalt(II) *n*-alkyl carboxylate (squares) and *n*-alkyl sulfate (circles) compounds.

(hydrated) to 9.3 Å (anhydrous), due to the loss of about two water molecules. A structural model may be proposed for the anhydrous phase on the basis of the X-ray diffraction results and taking into account the van der Waals spheres for the constitutive atoms [15,30]. The acetate anion is coordinated to cobalt(II) ion by the oxygen atom, and occupies the interlayer spacing with a head-to-tail arrangement. This model is very similar to that deduced for the copper(II) hydroxide acetate [31].

When the length of the coordinating anion (*n*-alkyl chain) becomes larger, a linear increase of the basal spacing *d* with the number of carbon atoms *n* is observed (Fig. 5). Focusing on the *n*-alkyl carboxylate series, *d* is related to *n* by the relation:  $d = d_0 + 1.27n \cos(\theta)$ .

From this relation, a single-layer packing [Fig. 4(a)] may be deduced, corresponding to a tilt angle of the chains,  $\theta = 52^\circ$ , with respect to the *c* axis [18,19]. The distance  $d_0 = 17.98$  Å stands for the sum of: (1) the size of the bridging carboxylate; (2) the distance between terminal methyl groups and the hydroxide layer; (3) the

van der Waals volume of water molecules; and (4) the inorganic layer thickness. The latter is deduced to be about 7.3 Å if water molecules occupy the space between the inorganic layer and terminal methyl groups. This model is clearly irrelevant for the hydroxide acetate, whose basal spacing (12.7 Å) is significantly lower than deduced for  $n=1$ .

Owing to the chemical composition of the above compounds, which agrees with  $\text{Co}_5(\text{OH})_8(\text{C}_n\text{H}_{2n+1}\text{COO})_2 \cdot z\text{H}_2\text{O}$  ( $z=2.5$  to  $3.8$ ), it can be assumed that the structure of the layers derives from the zinc analogue  $\text{Zn}_5(\text{OH})_8(\text{NO}_3)_2 \cdot 2\text{H}_2\text{O}$  [32].

The presence of tetrahedral sites for cobalt(II) ion is further pointed out from UV spectra. A structural model is proposed in Fig. 6. It consists of stacks of inorganic layers made up of cobalt(II) ions in octahedral and tetrahedral surroundings, the latter being located on each side of the median layers. The aliphatic chains are then connected through the carboxylate moieties to the Co(Td) metal ions, and occupy the space between layers with a tilt angle with respect to the  $c$  axis.

The  $n$ -alkyl sulfate series exhibits a somewhat different variation of the basal

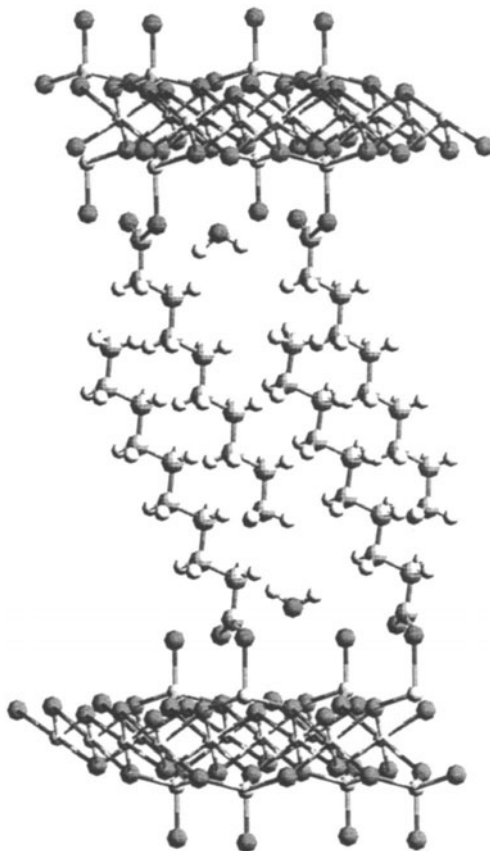


Fig. 6. Structural model for the layered cobalt(II)  $n$ -alkyl carboxylate compounds.



spacing with  $n$ . The linear dependence of  $d$ , given by  $d = 14.02 + 0.88n$ , agrees with a tilt angle  $\theta = 46^\circ$ .

In the same procedure as above, the thickness of the inorganic layer is shown to be 8.6 Å (without including water molecules), which may be compared to  $\text{Zn}_5(\text{OH})_8(\text{NO}_3)_2 \cdot 2\text{H}_2\text{O}$  (7.3 Å). The difference between both values (1.3 Å) is likely due to the water molecules, but their location cannot be explained as above ( $n$ -alkyl carboxylate series). According to the low density of aliphatic chains, the water molecules could occupy the space between the chains, close to the inorganic layers.

For that series, the chemical analysis gives a formulation  $\text{Co}_7(\text{OH})_{12}(\text{C}_n\text{H}_{2n+1}\text{SO}_4)_2 \cdot z\text{H}_2\text{O}$ , showing that the packing of octahedral and tetrahedral sites in the layers differs from the zinc hydroxide nitrate. Here, two in seven cobalt(II) ions occupy tetrahedral sites instead of two in five in the zinc hydroxide nitrate.

The magnetic behaviors of the cobalt(II) compounds  $\text{Co}_2(\text{OH})_4-x\text{X}_x \cdot z\text{H}_2\text{O}$ , with  $\text{X} = \text{C}_n\text{H}_{2n+1}\text{SO}_4^-$  or  $\text{C}_n\text{H}_{2n+1}\text{COO}^-$  are qualitatively similar. Fig. 7 shows the  $\chi T = f(T)$  variation for the  $n$ -alkyl carboxylate series. At high temperature, the  $\chi T$  values are nearly constant, in agreement with those expected for isolated cobalt(II) ion (from 2.5 to 3.0 cm<sup>3</sup> K mol<sup>-1</sup>). Upon cooling, a striking change of the magnetic properties is observed. The  $\chi T$  product shows a minimum in the range 90–110 K, which may be related to spin–orbit coupling effect or AF in-plane interactions, then a sharp increase indicating that a ferro- or ferrimagnetic ground-state is stabilized. The maximum value of  $\chi T$  increases from  $\sim 55$  cm<sup>3</sup> K mol<sup>-1</sup> to 220 cm<sup>3</sup> K mol<sup>-1</sup> as the basal spacing increases from 12.7 Å ( $n=1$ ) to 27.4 Å ( $n=12$ ). At very low temperature, the susceptibility depends strongly on the applied field: this effect is all the more pronounced as the basal spacing increases. Hysteresis cycles are observed for the  $n$ -alkyl compounds, with a large spontaneous magnetization and coercive field. The saturation value at 20 kOe ( $\sim 1\mu_B$  per mol Co) is lower than the expected one for cobalt(II) moment at low temperature ( $\sim 2\text{--}3\mu_B$  per mol Co). Owing to the

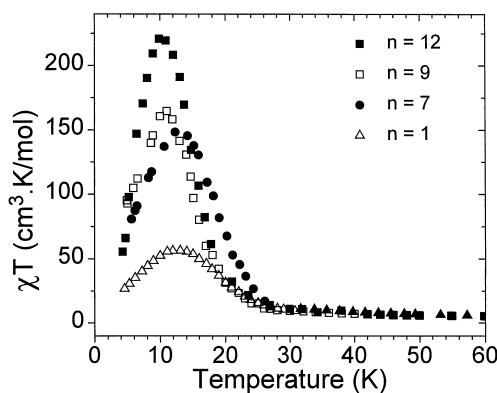


Fig. 7. Temperature dependence of the  $\chi T$  product for the layered cobalt(II)  $n$ -alkyl carboxylate compounds with increasing  $n$  values.

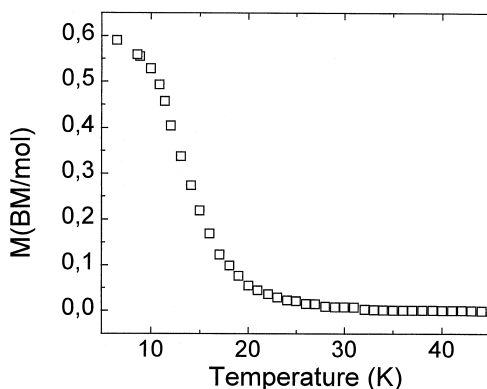


Fig. 8. Field-cooled magnetization measurement ( $H=200$  Oe) showing the occurrence of a long-range magnetic ordering for  $n=9$ .

structural findings and  $\chi T$  variation, it may be assumed that the ground-state is ferrimagnetic, due to uncompensated subnetworks involving cobalt(II) in Oh and Td symmetries.

Field-cooled magnetization measurements, for  $H=200$  Oe, confirm the stabilization of a net moment (Fig. 8). Below  $T_c$ , an out-of-phase signal, characteristic of a 3D ferromagnetic-like order, is observed by a.c. susceptibility measurements.

These results highlight the relationships between structures and magnetic properties in this series of layered compounds. A large change in magnetization is evidenced as a function of the basal spacing between the ferromagnetic layers. Note that a distinction has to be made between single-layered and double-layered  $n$ -alkyl compounds. However, these distinctions do not alter the relationship between the basal spacing and the magnetic behavior within a homologous series.

The role of hydrogen bonds appears to be negligible when either the distance between magnetic moments is very large or when aliphatic chains are involved. For  $\text{Co}_2(\text{OH})_{3.2}(\text{OAc})_{0.8} \cdot z\text{H}_2\text{O}$ , interactions due to hydrogen bonds may exist, but the distance between magnetic layers (9.3 Å and 12.7 Å) is apparently too large for antiferromagnetic interlayer interactions to be efficient. Such exchange mechanisms are also irrelevant in the case of  $\text{Co}_2(\text{OH})_{4-x}(\text{X})_x \cdot z\text{H}_2\text{O}$  with  $\text{X} = \text{C}_n\text{H}_{2n+1}\text{COO}^-$  or  $\text{C}_n\text{H}_{2n+1}\text{SO}_4^-$ .

Clearly, the question which dominates deals with the dimensionality of the magnetic network, in other words, to what extent two-dimensional long-range ordering may explain the observed behavior. Basically, the Ising anisotropy may promote two-dimensional ordering, but owing to the curves of magnetization, exhibiting the typical features of classical magnets, the ordering is most likely three-dimensional in the case of cobalt(II) compounds. For more insight into the actual dimensionality, copper(II) compounds characterized by isotropic spins have been investigated.

Series of layered copper(II) compounds  $\text{Cu}_2(\text{OH})_3(\text{X}) \cdot z\text{H}_2\text{O}$  ( $\text{X} = \text{C}_n\text{H}_{2n+1}\text{SO}_4^-$ ,  $\text{C}_n\text{H}_{2n+1}\text{COO}^-$ ) have been prepared by exchange reaction, according to the pro-

cedures reported above. In all cases, the X-ray diffraction patterns exhibit intense (00 $l$ ) reflections, in agreement with the layered-type structure of the materials.

For the  $\text{Cu}_2(\text{OH})_3(\text{C}_n\text{H}_{2n+1}\text{SO}_4) \cdot m\text{H}_2\text{O}$  series, the interlayer spacing increases linearly with the aliphatic chain length, according to the relationship  $d(\text{\AA}) = 12.01 + 1.27n$  (Fig. 9). This implies unambiguously that the  $n$ -alkyl chains are organized in a zip-like stacking [single layers, Fig. 4(a)] and most likely orientated normal to the inorganic layers. In this configuration, the terminal methyl groups of the alkyl chains exhibit hydrophobic interaction with the hydrogen atoms of the hydroxide layers.

The temperature dependent susceptibility for copper(II)  $n$ -alkyl sulfates is plotted as  $\chi T$  versus  $T$  in Fig. 10. At high temperature, the observed value is that expected for two copper(II) per mole ( $\sim 0.8 \text{ cm}^3 \text{ K mol}^{-1}$ ). At low temperature, the decrease of  $\chi T$  indicates that AF interactions dominate. Owing to the large separation between magnetic layers, 19.1  $\text{\AA}$  ( $n=6$ ) to 26.7  $\text{\AA}$  ( $n=12$ ), it can be stated that 2D short-range correlations are responsible for the observed behaviors. Slight structural modifications of the layers likely explain the difference between  $\chi T = f(T)$  variations.

Two series of layered hydroxide carboxylates  $\text{Cu}_2(\text{OH})_3(\text{C}_n\text{H}_{2n+1}\text{COO}) \cdot z\text{H}_2\text{O}$  have been isolated after one day and three days exchange reaction, respectively; a hydrated series ( $\alpha$ ) and an anhydrous series ( $\beta$ ), characterized by the same  $\text{Cu}/\text{OH}/\text{C}_n\text{H}_{2n+1}\text{COO}$  ratios [30,33].

The copper(II) hydroxide acetate obeys monoclinic symmetry, while monoclinic or hexagonal symmetry is evidenced for longer aliphatic chains, depending on the degree of ordering of the exchanged anion. The two different structural varieties,  $\alpha$  and  $\beta$ , are observed for the largest  $n$  values. For both series, the interlayer spacing varies linearly with the alkyl chain length ( $n$ ), according to the relationship  $d(\text{\AA}) = d_0 + 2.54n \cos \theta$  (Fig. 9), in agreement with a double-layer packing of the alkyl chains [Fig. 4(b)].

The temperature dependence of  $\chi T$  for the copper(II)  $n$ -alkyl carboxylates is illustrated in Fig. 11 for  $n=1$  (acetate) and  $n=7$ , which is representative of long-

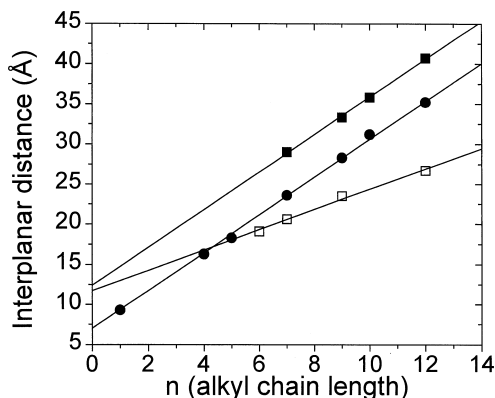


Fig. 9. Variation of the interlayer spacing as a function of  $n$  in copper(II)  $n$ -alkyl carboxylate (full squares and circles) and  $n$ -alkyl sulfate (open squares) compounds.

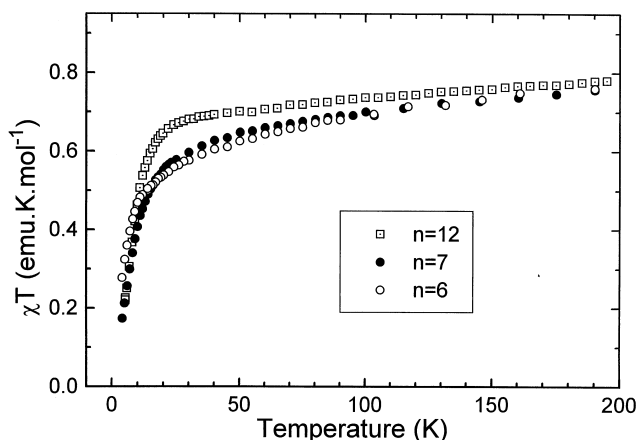


Fig. 10. Temperature dependence of the  $\chi T$  product for copper(II)  $n$ -alkyl sulfate compounds with increasing  $n$  values.

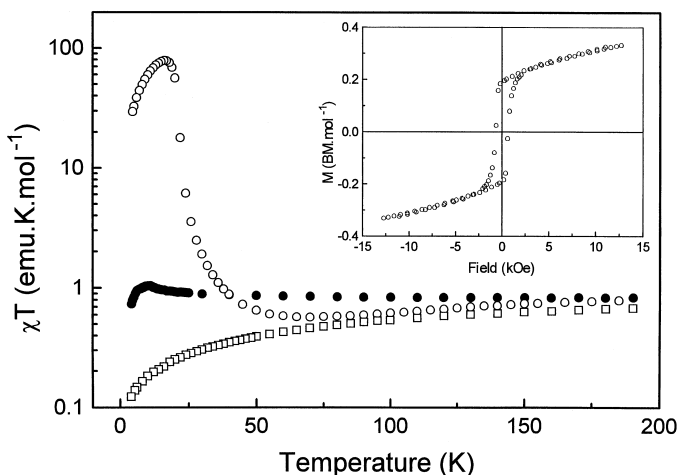


Fig. 11. Temperature dependence of  $\chi T$  for copper(II)  $n$ -alkyl carboxylates with  $n=1$  (full circles),  $n=7\alpha$  (open squares) and  $n=7\beta$  (open circles). Isothermal magnetization for the  $\beta$  phase is given in the inset.

chain compounds. Upon cooling, the hydroxide acetate shows a constant value of  $\chi T$ , then a slight increase up to  $1.0 \text{ cm}^3 \text{ K mol}^{-1}$  at 10 K, suggesting weak ferromagnetic (F) intralayer interactions. At lower temperature, the drop of  $\chi T$  indicates that interlayer AF interactions promote a 3D ordered state. Different behaviors are observed for the long-chain polymorphs  $\alpha$  and  $\beta$ . Whatever the  $n$  value, the  $\alpha$  compounds show a decrease of  $\chi T$  down to 2 K, denoting the antiferromagnetic character of the exchange couplings. In turn, the behavior of the  $\beta$  series differs drastically. Upon cooling, a decrease of  $\chi T$  is first observed down to a minimum at 60 K then a very sharp increase at lower temperature, pointing towards a ferrimag-

netic or canted spin arrangement within the copper(II) layers. The very large value of  $\chi T_{\text{max}}$  is the signature of a net magnetic moment in the ground-state [17,30,33].

The occurrence of long-range ferromagnetic order is illustrated by a characteristic hysteresis loop in the  $M(H)$  curve at  $T=4.2$  K (inset to Fig. 11). Similar behaviors are observed for the different  $\beta$  compounds, even for very large interlayer spacing (e.g. up to 40 Å for  $n=12$ ).

Finally, the magnetic study of these series of hybrid compounds shows that spectacular and unexpected behaviors may be observed, depending on the basal spacing. When alkyl sulfate groups are coordinated to copper(II) ions, the magnetic behavior is always antiferromagnetic. Alkyl carboxylate groups favor in turn either F or AF behaviors. As demonstrated for copper(II) exchange-coupled systems [34], a slight modification of the copper(II)–copper(II) oxo-bridges is likely responsible for the change in intralayer coupling.

#### 4. Very long-range ferromagnetic order

Owing to the nature of the ligands, the alkyl chains do not participate directly in the interlayer coupling, but noticeable change can result in the magnitude of the in-plane interaction, in particular for copper(II) compounds whose behavior is closely related to structural features.

It can be pointed out that: (1) antiferromagnetic in-plane correlations promote, for large basal spacing, an AF 2D short-range order; (2) for ferromagnetic in-plane interactions, the situation depends to a large extent on the interlayer spacing. For small spacing (less than 10 Å), the interlayer interactions via hydrogen bond superexchange pathways stabilize a 3D AF order, and a metamagnetic transition is observed in low field. When the spacing is made larger (large  $n$  values), the superexchange mechanisms can no longer be considered efficient. Nevertheless, the compounds exhibit a spontaneous magnetization and a characteristic hysteresis cycle. Ordering temperatures range between 21.2 and 19 K for  $n=7$  to 12 ( $c=28.8$  to 40.4 Å) for copper(II) compounds and between 16.5 and 22.7 K ( $c=9.3$  to 27.4 Å) for the cobalt(II) derivatives. Such large ferromagnetic ordering temperatures and their weak dependence on the interlayer spacing can hardly be related to superexchange interactions. In turn, they can be explained by considering dipolar through-space interactions between layers.

The strength of the electrostatic exchange and dipolar interaction energies between two discrete moments at a distance  $r$  apart decreases crudely as  $r^{-10}$  and  $r^{-3}$  respectively [35,36]. Clearly, the electrostatic interaction is by far the most important contribution for small  $r$  values but, in turn, becomes negligible compared with the dipole interaction for large distances.

Consider a two-dimensional ( $xy$ ) square lattice of spins  $S$ , coupled by ferromagnetic exchange interactions to their nearest neighbors. At absolute zero, the magnetic layer exhibits a ferromagnetic alignment of the spins due to exchange coupling, and the ground-state corresponds to the higher spin multiplicity. Upon increasing the temperature, the spins become correlated only on a finite distance  $\xi$ . For a 2D

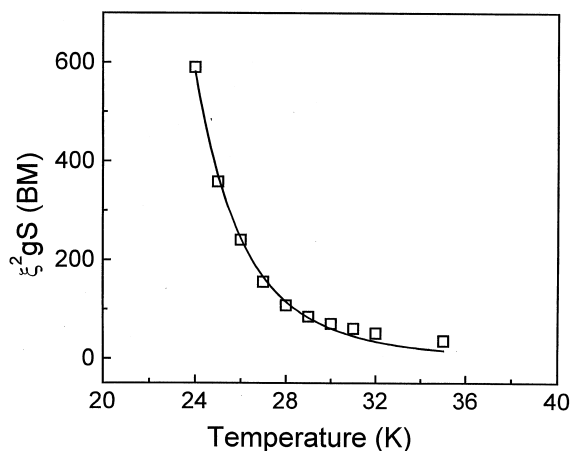


Fig. 12. Variation of  $\xi^2 g S$  upon cooling down for the  $n=7$  compound, determined from magnetization data above  $T_c$ .

Heisenberg ferromagnet, this is related to the exchange constant  $J$  and the spin value  $S$  by the relationship [37]:

$$\xi^2 = (JS/kT) \exp(4\pi JS^2/kT)$$

The exponential divergence of  $\xi$  is well illustrated in Fig. 12 by the temperature dependence of the effective paramagnetic moment  $\xi^2 g \mu_B S$ , deduced from magnetization data for the  $n=7$  copper(II) compound. It is well fitted in the paramagnetic region, just above  $T_c$ , using  $J=44$  K. As far as the actual exchange constant between copper(II) ions is concerned, this value should be renormalized to take into account the trigonal symmetry and the spin density of the real compound. This is achieved by scaling the moment density from the experimental value of the saturation magnetization. For instance, the lattice parameter of the square lattice equivalent to the experimental triangular lattice is  $5.7 \text{ \AA}$  for  $n=7$  ( $a=3.15 \text{ \AA}$ ).

The basic idea is that the dipole interaction between layers stacked along  $z$  leads to 3D ordering as soon as the in-plane correlation length  $\xi$  reaches a threshold value related to the interlayer spacing  $c$ . Because of the exponential divergence of  $\xi$ , the temperature for which the threshold is reached should depend only weakly on  $c$ , as experimentally observed. In order to minimize the dipole and anisotropy energies, the order between layers is expected to be ferromagnetic if  $z$  is the easy axis.

Considering that the interlayer spacing  $c$  is large compared to the in-plane lattice parameter  $a$ , it is assumed that:

- the in-plane correlation length is determined only by the in-plane exchange interaction;
- any exchange interaction between layers is negligible, and only through-space dipole coupling is available between moments located in different layers; and
- a small local anisotropy favors the spin orientation normal to the layers.

Accordingly, each layer is considered as a chess board with alternating spin-up and

spin-down squares, each one containing  $\xi^2$  spins. Each square is thus considered as a superspin, the moment of which is  $\xi^2 g \mu_B S = \xi^2 \mu$ .

The dipole field acting on a superspin due to all other superspins has been calculated according to the expression [36]:

$$H_{\text{dip}} = \langle \mu_z \rangle \sum_{ij} [1 - 3 \cos^2(\theta_{ij})] / r_{ij}^3$$

which takes into account the spatial extension of the superspins. The calculation converges rapidly for  $r$  values of the order of  $\xi$ . The above expression can be rewritten as:

$$H_{\text{dip}} = \lambda(\xi) \langle \mu_z \rangle$$

where  $\lambda$  is a coupling coefficient depending on the correlation length. Fig. 13 shows the variation of this coupling coefficient as a function of  $\xi$  for  $c/a=3$ , and an increasing number of interacting layers ( $L$ ).

In order to get a picture of the critical region, i.e. the transition to long-range order, a simple molecular field theory was considered, where the molecular field is given by the dipole field calculated above.

The temperature dependence of the spontaneous magnetization is then obtained, as usual, by solving the self-consistent set of equations:

$$\langle \mu_z \rangle = \mu [\coth(x) - 1/x] \quad \text{where} \quad x = \xi^2 \mu H_m / kT$$

$$H_m = \lambda(\xi) \langle \mu_z \rangle$$

With the knowledge of  $\xi(T)$  from the magnetization data above  $T_c$  [for  $n=7$  copper(II) compound], the expected variation of the spontaneous magnetization  $\langle \mu_z \rangle / \mu$  as a function of temperature can be computed (Fig. 14).

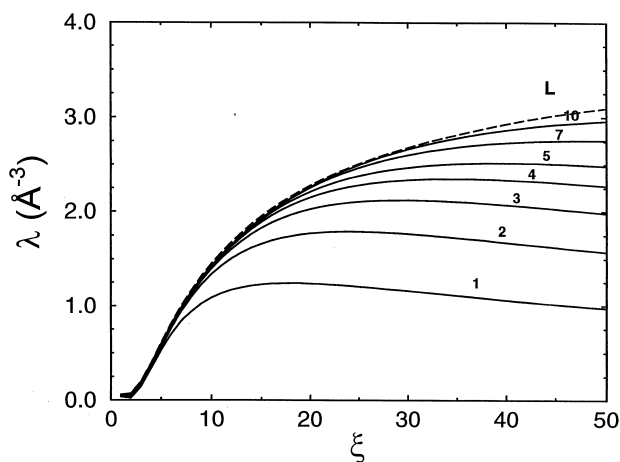


Fig. 13. Variation of the dipolar interaction coefficient  $\lambda(\xi)$  for  $c/a=3$ , and increasing number of interacting layers ( $2L$ ).

The critical temperature at which spontaneous magnetization occurs is shown to be about 19.4 K, which compares well with the experimental value  $T_c = 21.2$  K. It is noticed that a variation of  $c/a$  does not modify dramatically the critical temperature (less than 2 K for a doubling of  $c/a$ ), as observed experimentally. Actually, such changes of the length scale along  $z$  are compensated within a few Kelvin by the very fast variation of  $\xi$ . In turn, modifications of the in-plane exchange interaction  $J$ , that affects directly the thermal dependence of  $\xi$ , induce very significant variations of the long-range ordering temperature (Fig. 14).

This calculation demonstrates the key role of the dipolar interactions on the 3D ordering.

The comparison of the model with available experiments points out that dipole interactions between 2D ferromagnets with axial easy axis promote long-range 3D ferromagnetic order, even for very large spacing between the magnetic layers. Such coupling is efficient, compared to the classical AF exchange mechanism, as long as the bridging ligands do not participate in electronic transfers.

Finally, this result demonstrates that the design of molecular ferromagnets may involve complementary strategies. The choice of suitable bridging ligands to optimize the overlap between magnetic orbitals and accordingly the exchange interaction is clearly the pertinent way. However, the self-assembling of magnetic layers may also promote long-range magnetic correlations, and as a result 3D ordering.

To some extent, such systems are quite similar to Co/Ru or Co/Cu superlattices made of alternating magnetic and non-magnetic metal layers, even if the basic mechanism of the interactions differs. These hybrid layered compounds with tunable basal spacing thus appear promising for the design of new 3D ferromagnets [38].

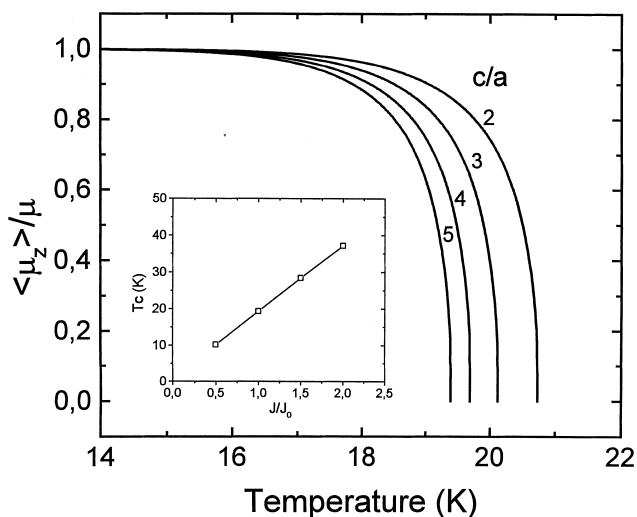


Fig. 14. Influence of the  $c/a$  ratio on the variation of the theoretical zero-field magnetization, using the divergence of  $\xi$ . The influence of the in-plane exchange interaction on the  $T_c$  value is given in the inset.  $J_0$  corresponds to the result of the fit for  $n=7$ .



## 5. Metal-radical layered magnets

In recent works, we have discussed for the first time the properties of hybrid organic–inorganic layered magnets made up of stacks of copper(II) or cobalt(II) hydroxide layers interleaved with organic radicals [14,30].

The benzoic acid-substituted imino-nitroxide (IMBA) radical has been used for stabilizing such hybrid systems. The free radical *p*-IMBA has been prepared by the sequence of reactions sketched in Fig. 15,<sup>2</sup> and characterized by classical methods (IR, UV–vis, mass spectrometry, and elemental analysis) as well as by single crystal structure study. A magnetic moment of  $1.73\mu_B$  was found at room temperature, showing that one free radical is well present per mole.

The most striking results have been obtained by exchange reaction of the anion  $\text{NO}_3^-$  by IMBA radical within the layered cobalt(II) hydroxide nitrate. The hybrid compound Co-rad, involving metal-radical subnetworks, has been achieved.

The comparison of the *h**k**l* reflections in the X-ray powder patterns shows that the layer structure and the metal–metal in-plane distance ( $a=3.15\text{ \AA}$ ) are unchanged. In turn, the 00*l* reflections shift from  $d_{001}=6.9\text{ \AA}$ , for the hydroxide nitrate, up to

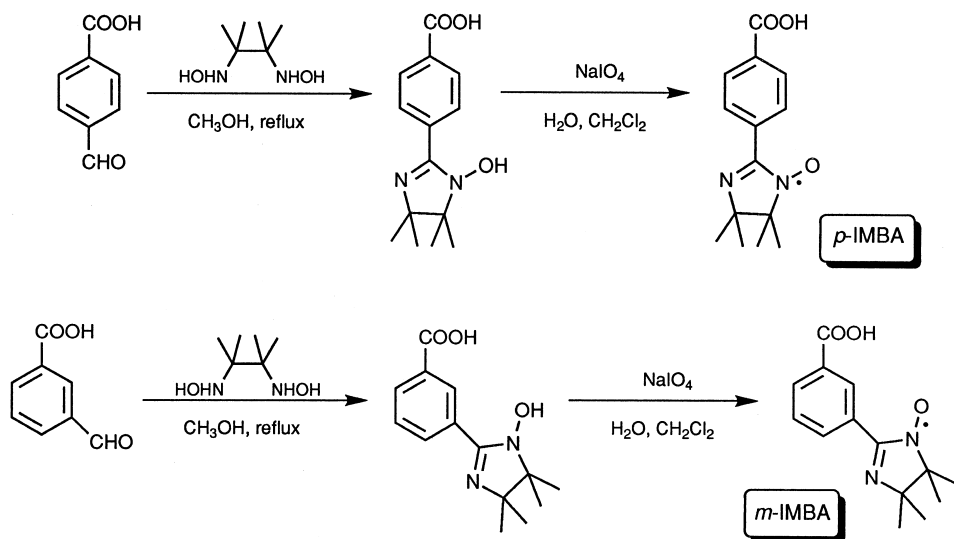


Fig. 15. General synthetic scheme followed for the preparation of imino-benzoic acids (IMBA) and their intermediates.

<sup>2</sup>According to a general method reported previously [14], the formyl derivatives are allowed to react with 2,3-bis(hydroxyamino)-2,3-dimethylbutane. The resulting hydroxyimidazolidines are oxidized with  $\text{NaIO}_4$  by phase transfer to afford the *p*- and *m*-imino-nitroxide derivatives in fair yields. The presence of an acid function within the aldehyde precursor facilitates the formation of the dehydrated intermediate (hydroxyimidazolidine versus dihydroxyimidazolidine in the classical cases). Both orange–red IMBA radicals are very stable and can be purified by chromatography on silica gel. Recrystallization from a dichloromethane/hexane solution gives red monocystals of *p*-IMBA.

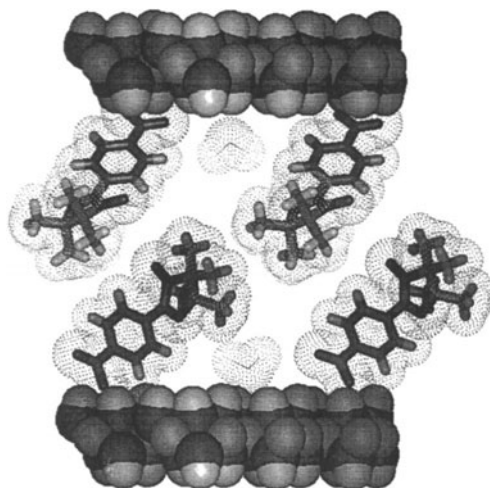


Fig. 16. Structural model for the hybrid layered compound Co-rad, showing the packing of IMBA radicals between the cobalt(II) layers.

about 20.2 Å for the exchanged compound, indicating a strong increase of the interlayer spacing, in agreement with the size and proposed stacking of the organic molecules (Fig. 16).

The magnetic behavior of the hybrid compound is illustrated in Fig. 17, as a plot of  $\chi T = f(T)$ . The exchange of nitrate anions by *p*-IMBA spin carriers induces a drastic change of the magnetic behavior. Upon cooling from room temperature, the  $\chi T$  product shows a minimum at around 65 K, and a strong divergence up to about

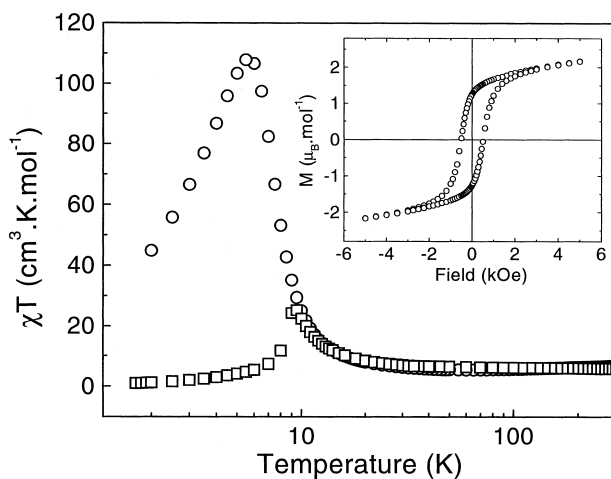


Fig. 17. Temperature dependence of  $\chi T$  for the hybrid compound Co-rad (circles). The behavior of the starting hydroxide nitrate (squares) is given for comparison. The variation of  $M(H)$  at 1.8 K is plotted in the inset.

$115 \text{ cm}^3 \text{ K mol}^{-1}$  below 10 K. Then, a maximum of  $\chi T$  occurs, but unlike the hydroxide nitrate, this compound does not order antiferromagnetically at all. The a.c. susceptibility measurements exhibit an out-of-phase signal which is the clear signature that a net moment is in the ground-state. The ordering temperature is found to be 6.0 K.

Field dependent magnetization data confirm these results (Fig. 17). The  $M(H)$  curve exhibits a hysteresis loop characteristic of a ferromagnetic-like 3D order. At 1.8 K, the coercive field is found to be 330 Oe, and the saturation magnetization  $3.5\mu_{\text{B}} \text{ mol}^{-1}$ . These results, together with those of the hybrid *n*-alkyl carboxylates, point to a model of ferrimagnetic cobalt(II) layer coupled to IMBA radicals through the  $\pi$  electrons of bridging ligands.

As expected, the EPR signal of the radical is located close to the free electron  $g$ -value at room temperature (Fig. 18). As observed in various radical-based magnets in the paramagnetic regime, the linewidth increases continuously and moderately, and the position of the resonance line, i.e. the  $g$ -factor, remains nearly unchanged from room temperature down to  $T_c$ . Drastic changes occur close to  $T_c$ , namely a strong broadening of the EPR signal and a large shift of the resonance. Therefore, the organic radical is actually proving the cooperative alignment of the neighboring cobalt(II) moments. The shift of the radical resonance means that the resonance field is no longer the applied Zeeman field. The exchange interaction between (i) radical spins,  $J_{\pi-\pi}$ , and (ii) radical and cobalt spins,  $J_{\pi-\text{Co}}$ , must be considered. None of these is large enough to give striking effects at room temperature, e.g. strong exchange narrowing or line broadening due to fast relaxation processes. However, as  $T_c$  is smaller in the radical-based compounds than for *n*-alkyl carboxylate derivatives, it appears that the sandwiched radical layer is actually counteracting the driving interaction for the bulk ferromagnetic ordering.

The dipolar interaction  $H_{\text{dip}}$  is assumed as the driving interaction for the set-up

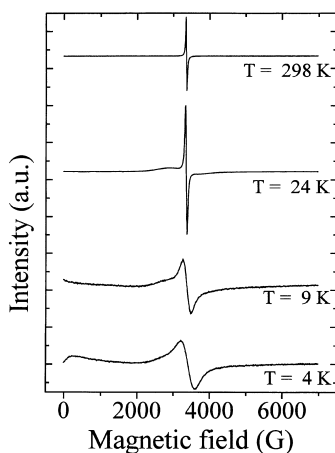


Fig. 18. X-band EPR spectra of Co-rad showing the strong broadening of the radical signal when approaching  $T_c$ .

of bulk ferromagnetism, as demonstrated above. It involves the in-plane spin–spin correlation function, which diverges critically as the layers are ordering, thus promoting bulk ferromagnetism. It can be stated that the radical spins do not simply line up within the internal field created upon ordering the cobalt(II) layers, otherwise the net magnetic moment would increase up to saturation more rapidly for the radical-based compound. The lowering of  $T_c$  with respect to *n*-alkyl carboxylate derivatives is likely due to the exchange interaction  $J_{\pi-\text{Co}}$ , confirming the existence of magnetic interactions between the organic and inorganic subnetworks, as evidenced from magnetic susceptibility experiments. For the first time, it is evidenced that 3D long-range ferromagnetism may occur in a hybrid metal–radical layered compound.

## 6. Concluding remarks

It is demonstrated in this work that self-assembled stacks of organic–inorganic subnetworks may promote very long-range magnetic correlations. Thus, a 3D ferromagnetic order is observed between copper(II) layers as far as 40 Å, illustrating the key role of dipolar interactions. These are also relevant in the metal–radical compounds, even if the organic (radical) and inorganic [cobalt(II)] spins are likely coupled through the  $\pi$ -system of the benzoic acid. The present result points to the fact that the divergence of the correlation length, and as a result the mean spin value within the ferromagnetic layers, is the important feature to promote the dipolar effects responsible for the 3D ordering.

In this respect, this family of layered hybrid systems differs basically from the classical radical-based molecular compounds (namely, radical complexed to metal ions), and appears very promising for the design of new kinds of ferromagnets.

## Acknowledgements

The authors thank Dr. P. Turek, from the Institut Charles Sadron (Strasbourg), for EPR experiments and helpful discussions on the results.

## References

- [1] J.S. Miller, A.J. Epstein, W.M. Reiff, *Chem. Rev.* 88 (1988) 201.
- [2] D. Gatteschi, O. Kahn, J.S. Miller, F. Palacio (Eds.), *Magnetic Molecular Materials*, Kluwer, Dordrecht, 1991.
- [3] O. Kahn (Ed.), *Molecular Magnetism*, VCH, Weinheim, 1993.
- [4] A. Caneschi, D. Gatteschi, J.P. Renard, P. Rey, R. Sessoli, *Inorg. Chem.* 28 (1989) 2940.
- [5] A. Caneschi, D. Gatteschi, P. Rey, R. Sessoli, *Inorg. Chem.* 30 (1991) 3936.
- [6] A. Caneschi, D. Gatteschi, J. Laugier, P. Rey, R. Sessoli, *J. Am. Chem. Soc.* 110 (1988) 2795.
- [7] K. Inoue, H. Iwamura, *J. Am. Chem. Soc.* 116 (1994) 3173.
- [8] P. Gülich, *Mol. Cryst. Liq. Cryst.* 305 (1997) 17 and references cited therein

- [9] Y. Sano, M. Tanaka, N. Koga, K. Matsuda, H. Iwamura, P. Rabu, M. Drillon, *J. Am. Chem. Soc.* 119 (1997) 8246.
- [10] M. Kurmoo, A.W. Graham, P. Day, S. Coles, M.B. Hursthouse, J.L. Caulfield, J. Singleton, F.L. Pratt, W. Hayes, L. Ducasse, P. Guionneau, *J. Am. Chem. Soc.* 117 (1995) 12209.
- [11] E. Coronado, J.R. Galan-Mascaros, C. Gimenez-Saiz, C.J. Gomez-Garcia, in: O. Kahn (Ed.), *Magnetism: A Supramolecular Function*, NATO ASI Series C, vol. 486, Kluwer Academic, Dordrecht, 1996, p. 28.
- [12] R. Clément, P.G. Lacroix, D. O'Hare, J. Evans, *Adv. Mater.* 6 (1995) 794.
- [13] S. Bénard, P. Yu, T. Coradin, E. Rivière, K. Nakatani, R. Clément, *Adv. Mater.* 9 (1997) 981.
- [14] M. Drillon, C. Hornick, V. Laget, P. Rabu, F.M. Romero, S. Rouba, G. Ulrich, R. Ziessel, *Mol. Cryst. Liq. Cryst.* 273 (1995) 125.
- [15] V. Laget, S. Rouba, P. Rabu, C. Hornick, M. Drillon, *J. Magn. Magn. Mater.* 154 (1996) L7.
- [16] P. Rabu, S. Rouba, V. Laget, C. Hornick, M. Drillon, *J. Chem. Soc., Chem. Commun.* (1996) 1107.
- [17] W. Fujita, K. Awaga, *Inorg. Chem.* 35 (1996) 1915.
- [18] M. Meyn, K. Beneke, G. Lagaly, *Inorg. Chem.* 32 (1993) 1209.
- [19] M. Meyn, K. Beneke, G. Lagaly, *Inorg. Chem.* 29 (1990) 5201.
- [20] M. Bujoli-Doeuff, L. Force, V. Gadet, M. Verdaguer, K. el Malki, A. de Roy, J.P. Besse, J.P. Renard, *Mater. Res. Bull.* 26 (1991) 577.
- [21] S. Yamanaka, T. Sako, K. Seki, M. Hattori, *Solid State Ion.* 53–56 (1992) 527.
- [22] L.J. de Jongh, A.R. Miedema, *Adv. Phys.* 23 (1974) 1.
- [23] P. Rabu, S. Angelov, P. Legoll, M. Belaiche, M. Drillon, *Inorg. Chem.* 32 (1993) 2463.
- [24] T. Takada, Y. Bando, M. Kiyama, H. Miyamoto, T. Sato, *J. Phys. Soc. Jpn.* 21 (1966) 2745.
- [25] M. Soraï, A. Kosaki, H. Suga, S. Seki, *J. Chem. Thermodynam.* 1 (1969) 119.
- [26] L.J. De Jongh (Ed.), *Magnetic Properties of Layered Transition Metal Compounds*, Kluwer, Dordrecht, 1990.
- [27] G.G. Linder, M. Atanasov, J. Pebler, *J. Solid State Chem.* 116 (1995) 1.
- [28] H. Heffenberger, *Z. Krist.* 165 (1983) 127.
- [29] S. Rouba, P. Rabu, E. Ressouche, L.-P. Regnault, M. Drillon, *J. Magn. Magn. Mater.* 163 (1996) 365.
- [30] V. Laget, P. Rabu, C. Hornick, F.M. Romero, R. Ziessel, P. Turek, M. Drillon, *Mol. Cryst. Liq. Cryst.* 305 (1997) 291.
- [31] N. Masciocchi, E. Corradi, A. Sironi, G. Moretti, G. Minelli, P. Porta, *J. Solid State Chem.* 131 (1997) 252.
- [32] M. Louër, D. Louër, D. Grandjean, *Acta Crystallogr. B* 29 (1973) 1696.
- [33] V. Laget, M. Drillon, C. Hornick, P. Rabu, P. Turek, R. Ziessel, *J. Alloys Compounds* 262 (1997) 423.
- [34] W.E. Hatfield, in: R.D. Willett, D. Gatteschi, O. Kahn (Eds.), *NATO ASI Series C* 140, Reidel, Dordrecht, 1985, p. 555.
- [35] D. Bloch, *J. Phys. Chem. Solids* 27 (1966) 881.
- [36] N.W. Aschcroft, N.D. Mermin, *Solid State Physics*, Hold-Saunders Int. Ed., 1981.
- [37] M. Takahashi, *Phys. Rev. Lett.* 58 (1987) 168.
- [38] R. Clément, *Science* 263 (1993) 658.